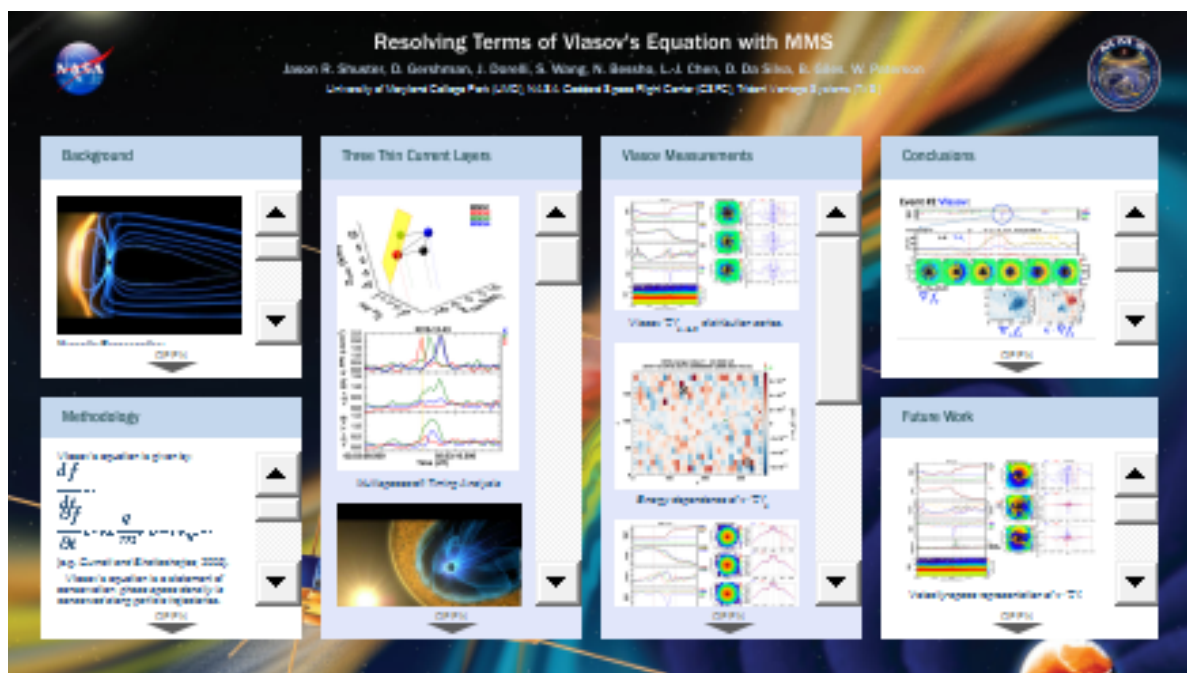


# Resolving Terms of Vlasov's Equation with MMS



Jason R. Shuster, D. Gershman, J. Dorelli, S. Wang, N. Bessho, L.-J. Chen, D. Da Silva, B. Giles, W. Paterson

University of Maryland College Park (UMD), NASA's Goddard Space Flight Center (GSFC), Trident Vantage Systems (TVS)



PRESENTED AT:

## BACKGROUND

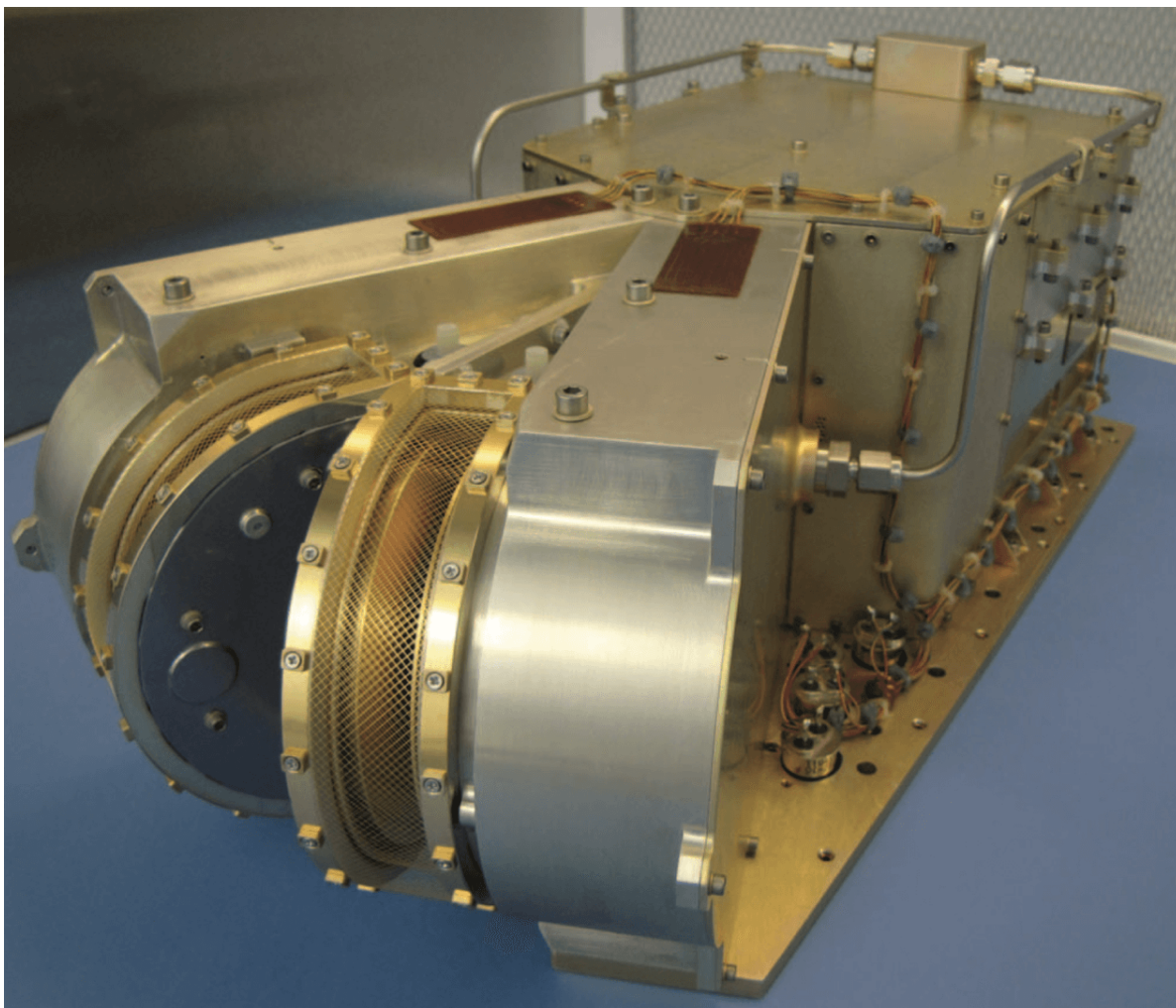
[VIDEO] [https://www.youtube.com/embed/i\\_x3s8ODaKg?feature=oembed&fs=1&modestbranding=1&rel=0&showinfo=0](https://www.youtube.com/embed/i_x3s8ODaKg?feature=oembed&fs=1&modestbranding=1&rel=0&showinfo=0)

### **Magnetic Reconnection**

How can magnetic reconnection occur in a collisionless plasma? This outstanding plasma physics mystery fueled the successful launch of NASA's MMS mission. The primary science goal of MMS is to reveal the electron-scale, three-dimensional structure and dynamics of the elusive electron diffusion region (EDR) believed to hold the key to the reconnection puzzle.

### **Vlasov's Equation and MMS**

Vlasov's equation is held by many to be the most important equation in all of plasma physics. This equation, also known as the collisionless Boltzmann equation, is employed to describe the motion of collisionless plasmas, such as those occurring naturally in Earth's magnetic environment, near the Sun, and throughout the solar system. Rather than assuming the plasma is a fluid, as in the framework of MHD (magnetohydrodynamics), the Vlasov equation treats the plasma *kinetically*, accounting for the motions of individual plasma particles. NASA's revolutionary Magnetospheric Multiscale (MMS) four-spacecraft mission is equipped with ground-breaking instrumentation capable of detecting these kinetic plasma features at unprecedented temporal and spatial resolution, faster than ever before achieved: MMS's Fast Plasma Investigation (FPI) captures fully three-dimensional electron moments every 30 milliseconds and ion moments every 150 milliseconds [Pollock *et al.*, 2016]. The unprecedented spatiotemporal resolution of MMS enables direct measure terms in Vlasov's equation for the first time. Thus, we are now able to test predictions of Vlasov's equation and plasma kinetic theory against direct observations from Earth's magnetosphere to see if we really understand how plasma behaves kinetically!



*Dual Electron Spectrometers (DES)*

[Collinson *et al.*, 2012: Figure 1]

*Additional Information*

\* Magnetospheric Multiscale Mission (<http://mms.gsfc.nasa.gov/>)

\* FPI Data Visualizer (<http://fpi.gsfc.nasa.gov/>)

\* Instruments onboard MMS ([http://www.nasa.gov/mission\\_pages/mms/spacecraft/mms-instruments.html](http://www.nasa.gov/mission_pages/mms/spacecraft/mms-instruments.html))

[VIDEO] <https://www.youtube.com/embed/gBK8n9r3Y7Y?feature=oembed&fs=1&modestbranding=1&rel=0&showinfo=0>  
*Demonstration of the new FPI Data Visualizer tool.*

## METHODOLOGY

Vlasov's equation is given by:

$$\frac{df}{dt} = 0$$

$$\frac{\partial f}{\partial t} + \mathbf{v} \cdot \nabla f + \frac{q}{m} (\mathbf{E} + \mathbf{v} \times \mathbf{B}) \cdot \nabla_{\mathbf{v}} f = 0$$

[e.g. *Gurnett and Bhattacharjee*, 2005].

Vlasov's equation is a statement of conservation: *phase space density is conserved along particle trajectories*. Additionally, Vlasov's equation can also be derived as a continuity equation for six-dimensional phase space.

We began an initial search of the MMS database for current sheets satisfying two primary criteria:

- (1)  $2 \text{ cm}^{-3} < n < 50 \text{ cm}^{-3}$ , and
- (2)  $|J_{\perp}| > 1.0 \text{ } \mu\text{A/m}^2$ .

With these criteria, we identified nearly ~2,000 candidate events. Three of these are featured in this presentation.

For computing gradients of phase space density measurements needed to approximate terms of Vlasov's equation from MMS data, we used the following formulae.

We applied the linear gradient approximation (1st order Taylor series expansion) to each FPI pixel (Q) measurement:

$$Q_2 \approx Q_1 + \frac{\partial Q}{\partial x} \Delta x_{21} + \frac{\partial Q}{\partial y} \Delta y_{21} + \frac{\partial Q}{\partial z} \Delta z_{21}$$

$$Q_3 \approx Q_1 + \frac{\partial Q}{\partial x} \Delta x_{31} + \frac{\partial Q}{\partial y} \Delta y_{31} + \frac{\partial Q}{\partial z} \Delta z_{31}$$

$$Q_4 \approx Q_1 + \frac{\partial Q}{\partial x} \Delta x_{41} + \frac{\partial Q}{\partial y} \Delta y_{41} + \frac{\partial Q}{\partial z} \Delta z_{41}$$

Inverting the resulting matrix equation, we can approximate linear gradients  $df/dx$ ,  $df/dy$ , and  $df/dz$ , which can be projected into any desired direction (e.g. field-aligned coordinates).



$$\begin{bmatrix} (x_2 - x_1) & (y_2 - y_1) & (z_2 - z_1) \\ (x_3 - x_1) & (y_3 - y_1) & (z_3 - z_1) \\ (x_4 - x_1) & (y_4 - y_1) & (z_4 - z_1) \end{bmatrix} \cdot \begin{bmatrix} \frac{\partial f}{\partial x} \\ \frac{\partial f}{\partial y} \\ \frac{\partial f}{\partial z} \end{bmatrix} = \begin{bmatrix} f_2 - f_1 \\ f_3 - f_1 \\ f_4 - f_1 \end{bmatrix}$$

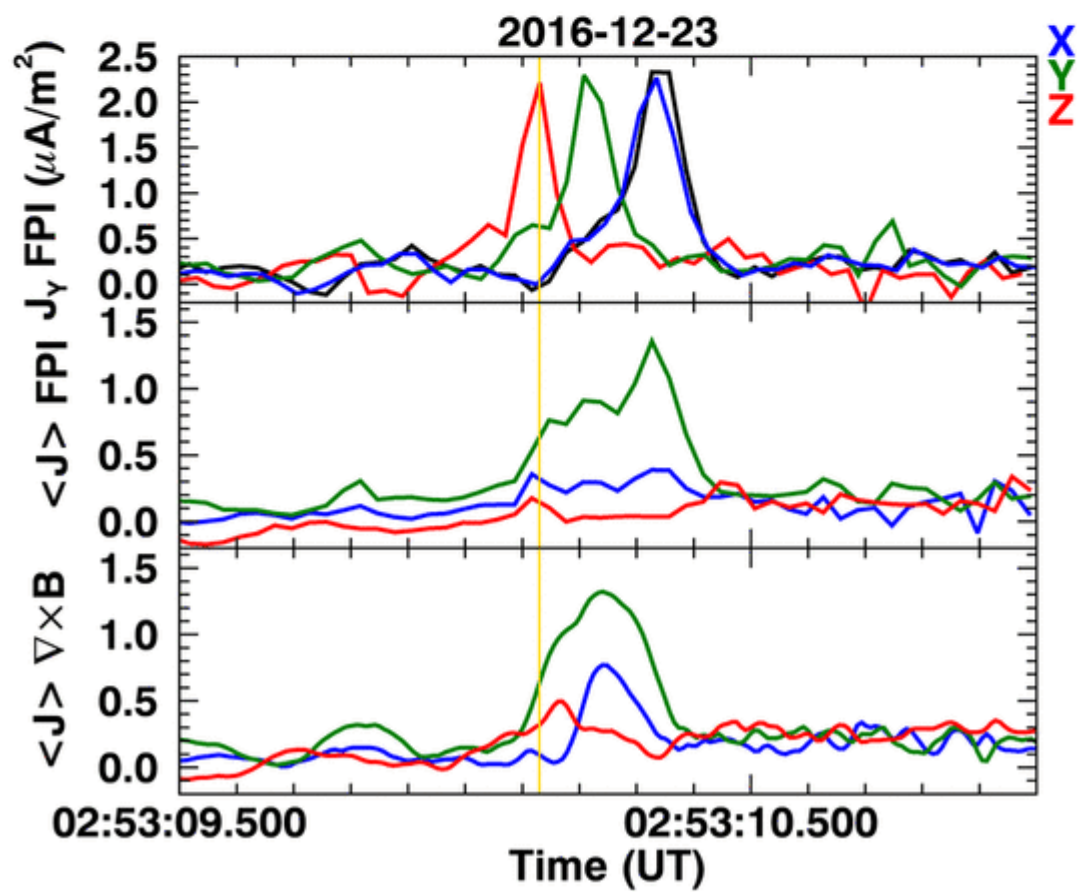
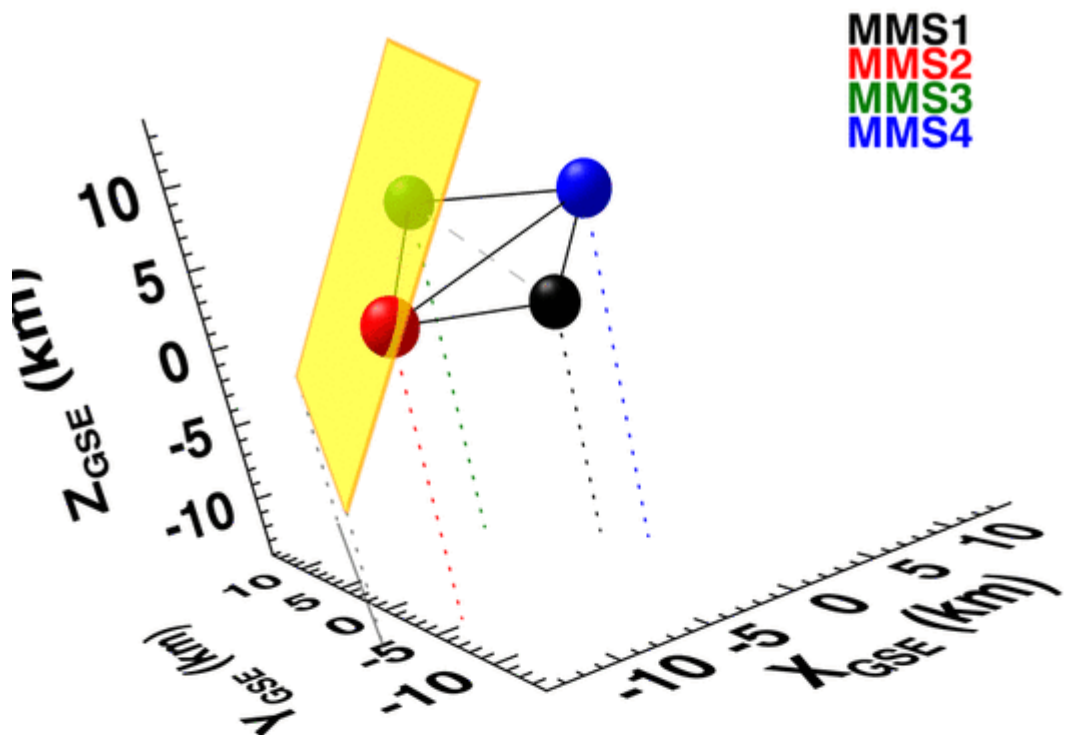
Once the gradients have been approximated, we can compute quantities such as  $\mathbf{v} \cdot \nabla f_e$ , noting that here  $\mathbf{v}$  is not the bulk velocity, but rather the phase-space velocity coordinate.

$$(\mathbf{v} \cdot \nabla f)^{i,j,k} = v_x^{i,j,k} \cdot \frac{\partial f(E_i, \theta_j, \phi_k)}{\partial x} + v_y^{i,j,k} \cdot \frac{\partial f(E_i, \theta_j, \phi_k)}{\partial y} + v_z^{i,j,k} \frac{\partial f(E_i, \theta_j, \phi_k)}{\partial z}.$$

Similarly, we can approximate the velocity-space gradients from single-spacecraft measurements as well:

$$(\nabla_{\mathbf{v}} f)^{i,j,k} = \frac{\partial f(E_i, \theta_j, \phi_k)}{\partial v} \hat{\mathbf{r}} + \frac{1}{v_i} \frac{\partial f(E_i, \theta_j, \phi_k)}{\partial \theta} \hat{\boldsymbol{\theta}} + \frac{1}{v_i \sin(\theta_j)} \frac{\partial f(E_i, \theta_j, \phi_k)}{\partial \phi} \hat{\boldsymbol{\phi}}.$$

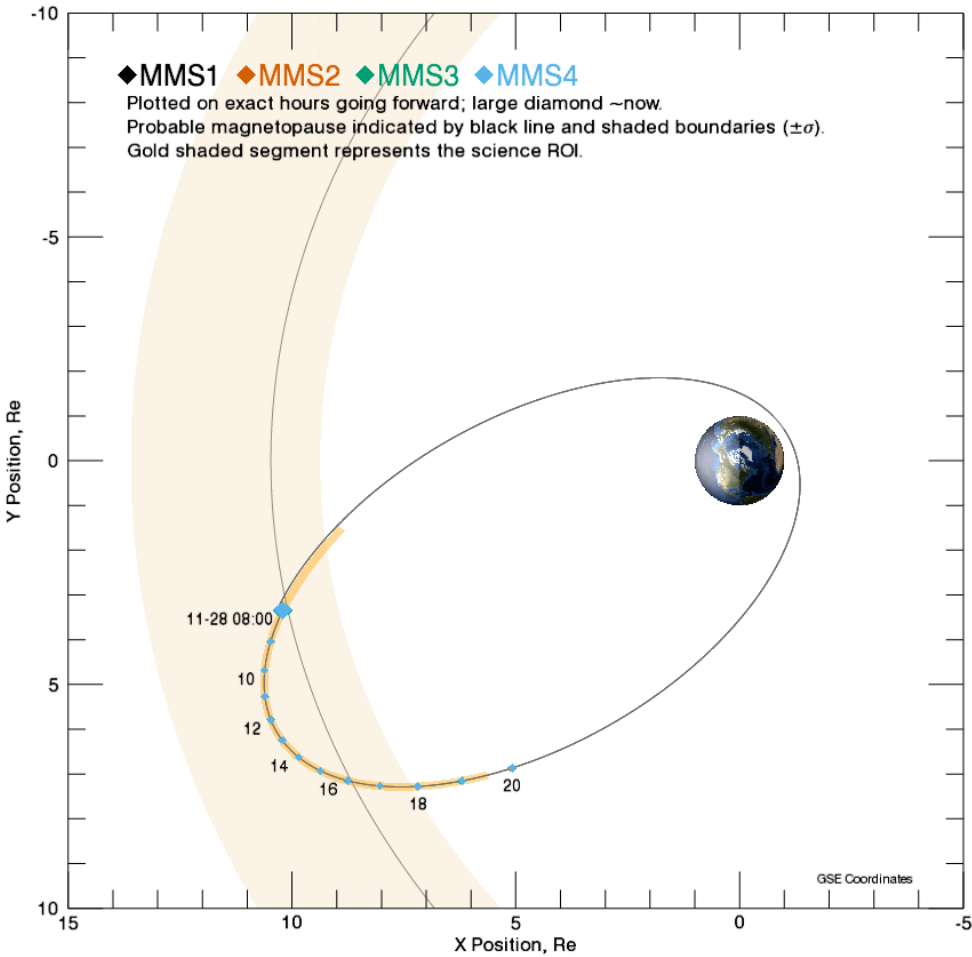
## THREE THIN CURRENT LAYERS



Multispacecraft Timing Analysis

[VIDEO] <https://www.youtube.com/embed/LX12E0-1XXw?feature=oembed&fs=1&modestbranding=1&rel=0&showinfo=0>  
Animation illustrating the Earth's magnetopause, the boundary between magnetospheric and turbulent magnetosheath plasma.

MMS Location for 2016-11-28 08:00:00 UTC



MMS orbit on 11/28/2016

Event #	Date & Time	Speed*	Thickness (0.3 to 0.5 sec) Local d <sub>e</sub> : 1.5 km	Electron Crescent?	MSP Electric Field Waves?
#1.	11/28/2016 07:32:17.334	30 km/s	9 to 15 km 6 to 10 d <sub>e</sub>	No	Yes
#2.	12/23/2016 02:53:10.327	50 km/s	15 to 27 km 10 to 16 d <sub>e</sub>	Yes	Yes
#3.	12/27/2016 03:39:15.835	55 km/s	16 to 27 km 10 to 18 d <sub>e</sub>	No	Yes

Event #	Date & Time	Shear Angle** $\theta$	$ B_2  /  B_1 $ Ratio	$\Delta\beta_e = \beta_{e1} - \beta_{e2}$ ***
<b>#1.</b>	<b>11/28/2016</b> 07:32:17.334	<b>22°</b>	23.9nT / 9.7nT = <b>2.5</b>	3.28 – 0.41 = <b>2.87</b>
<b>#2.</b>	<b>12/23/2016</b> 02:53:10.327	<b>14°</b>	34.0nT / 9.6nT = <b>3.5</b>	4.11 – 0.26 = <b>3.85</b>
<b>#3.</b>	<b>12/27/2016</b> 03:39:15.835	<b>63°</b>	41.0nT / 10.8nT = <b>3.8</b>	4.74 – 0.17 = <b>4.57</b>

#### Event Characteristics

\*Speed of current sheet determined from multispacecraft timing analysis.

\*\*Shear angles across the current layers computed over roughly a two-second interval:  $\theta = \cos^{-1}(\mathbf{b}_1 \cdot \mathbf{b}_2)$

\*\*\*MSH-side (smaller  $|B|$ ) is "1", and MSP-side (larger  $|B|$ ) is "2".

#### Three Thin Current Sheets

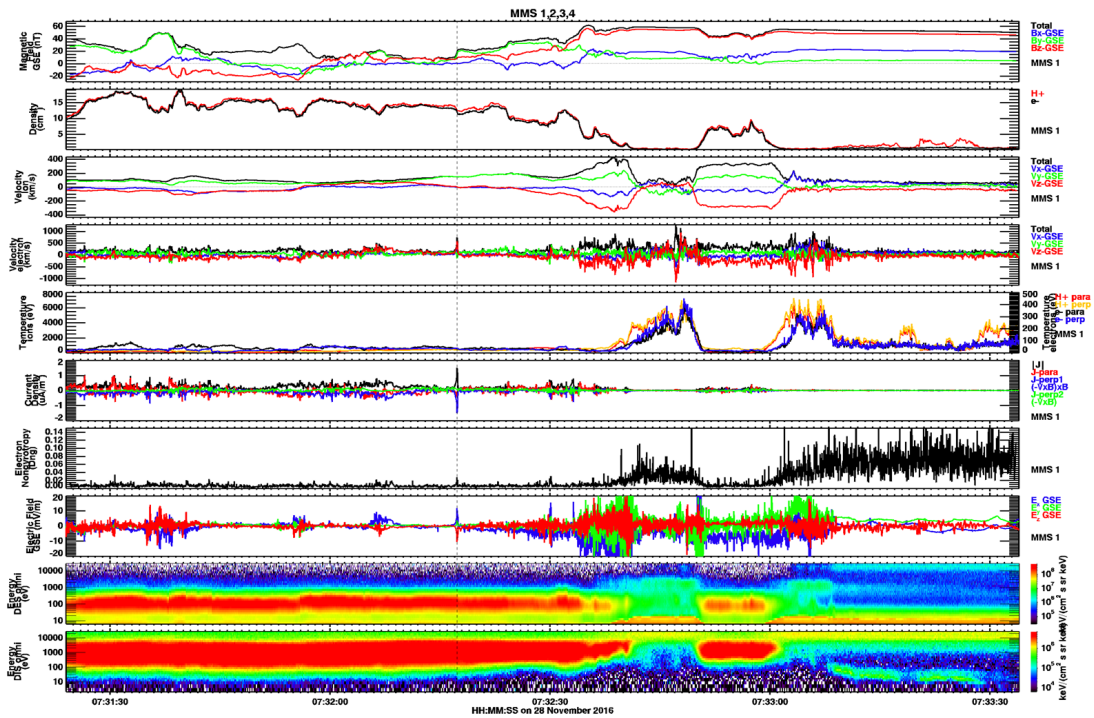
Event #1: 11/28/2016

Event #2: 12/23/2016

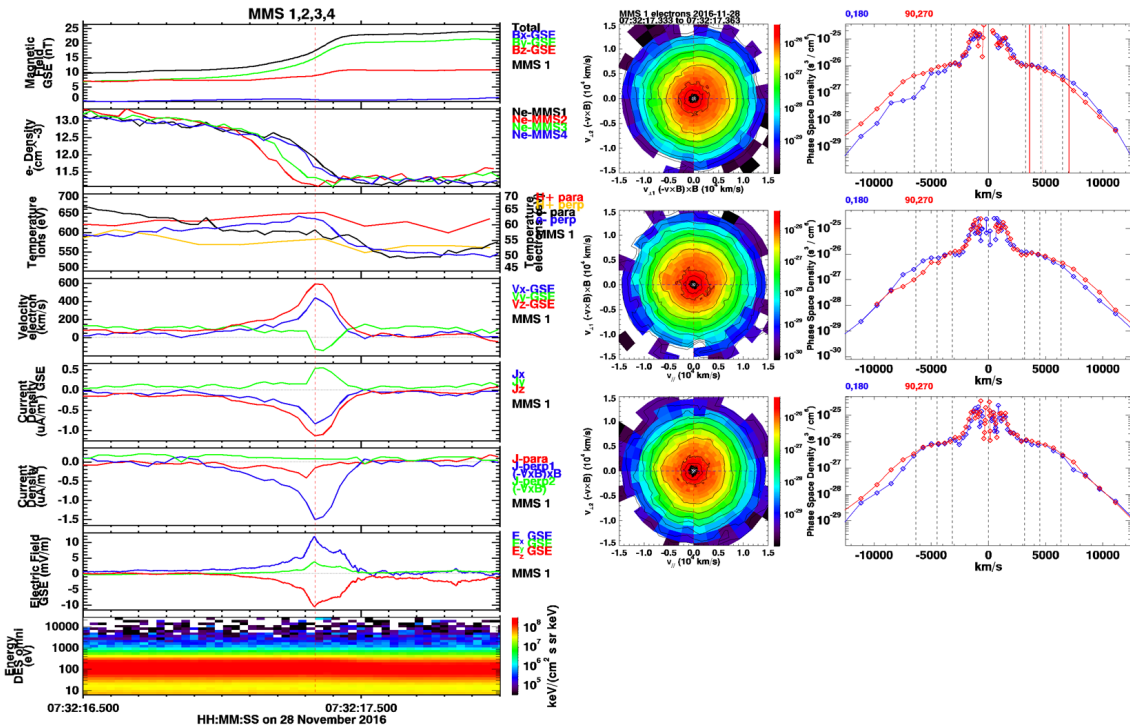
Event #3: 12/27/2016

Plasma parameters for each event:

Event #1: Burst Interval Overview

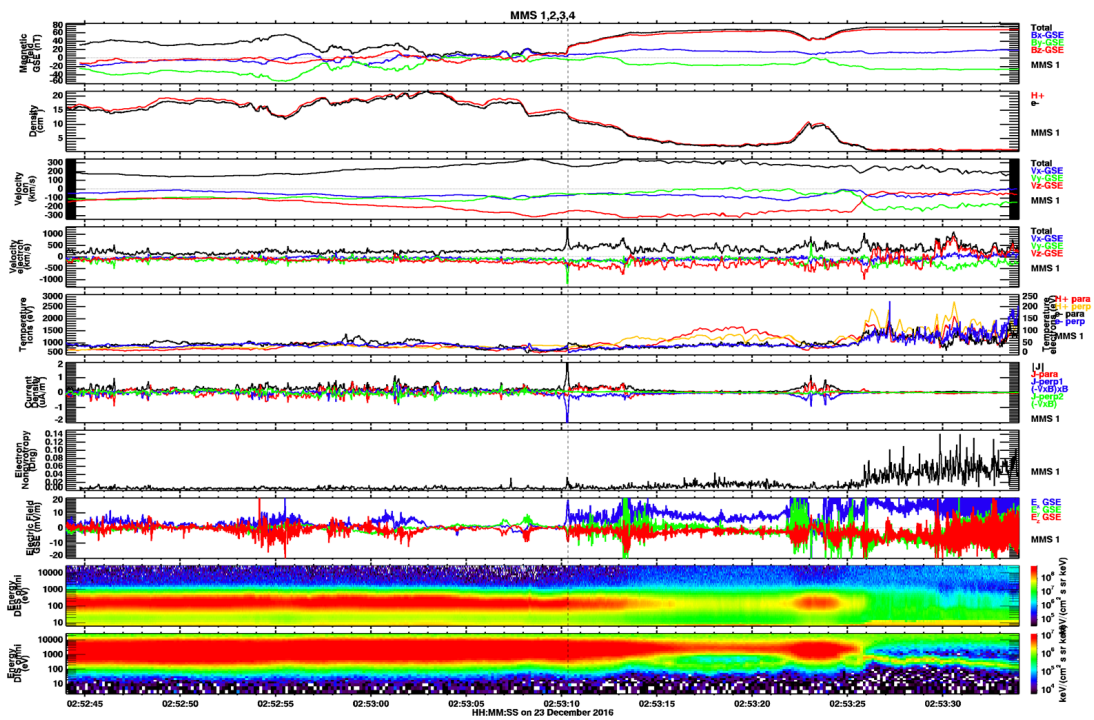


Event #1: Zoom

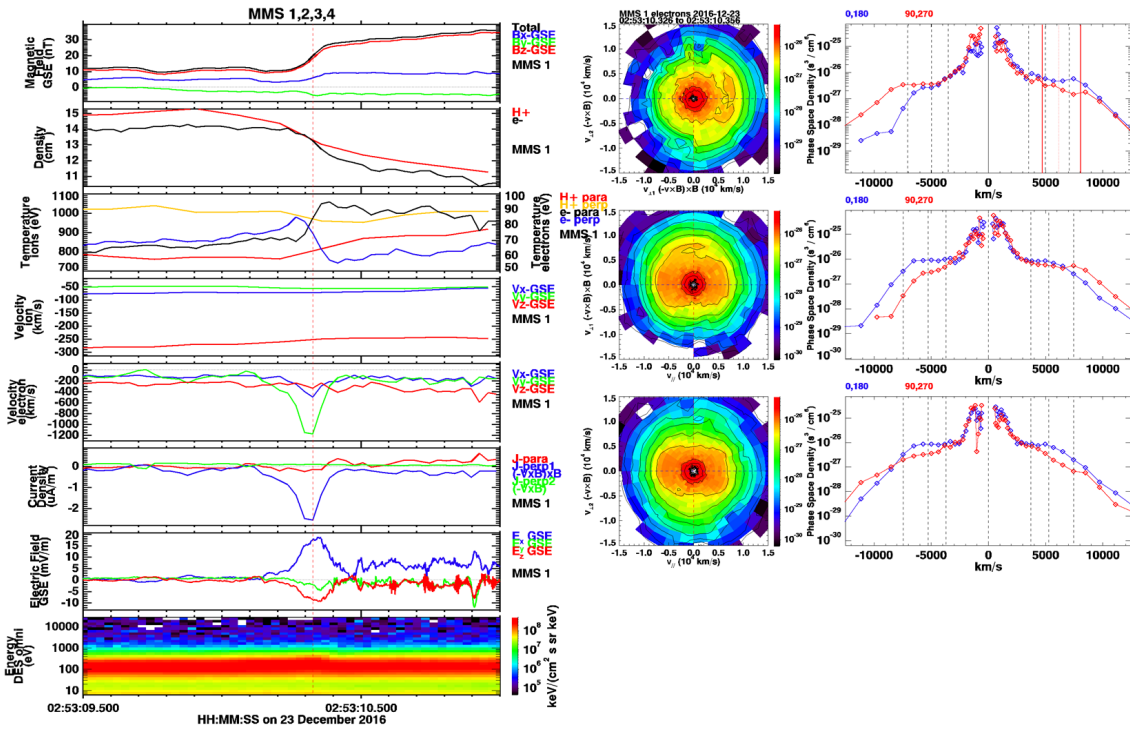


Event #2: Burst Interval Overview

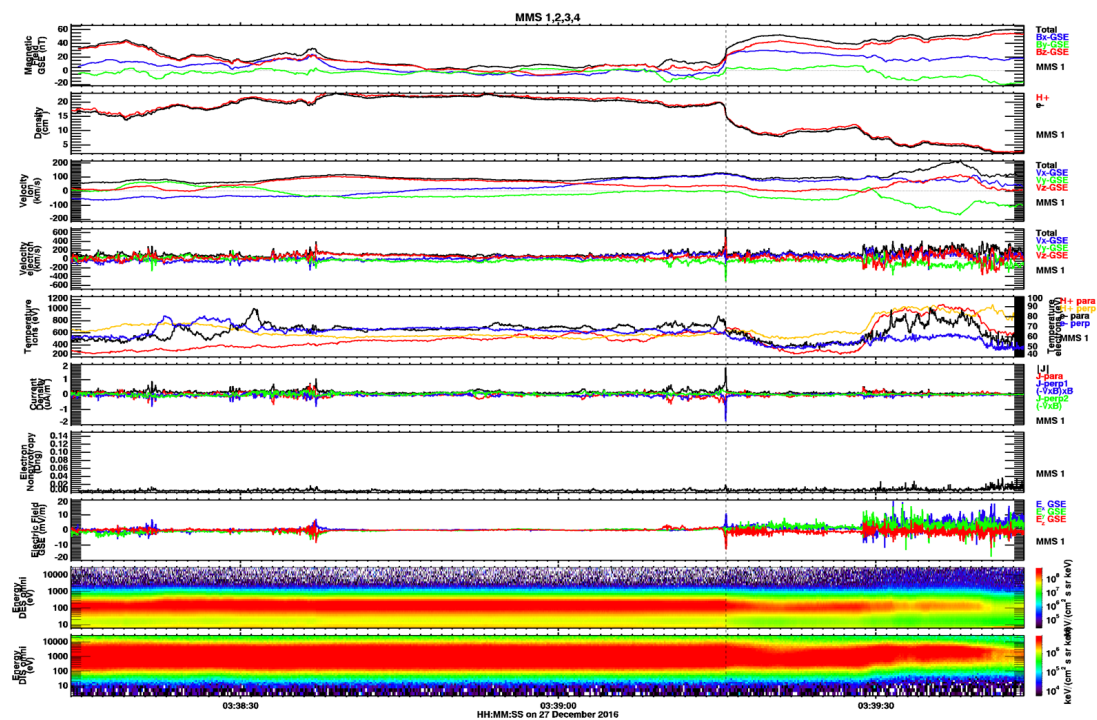




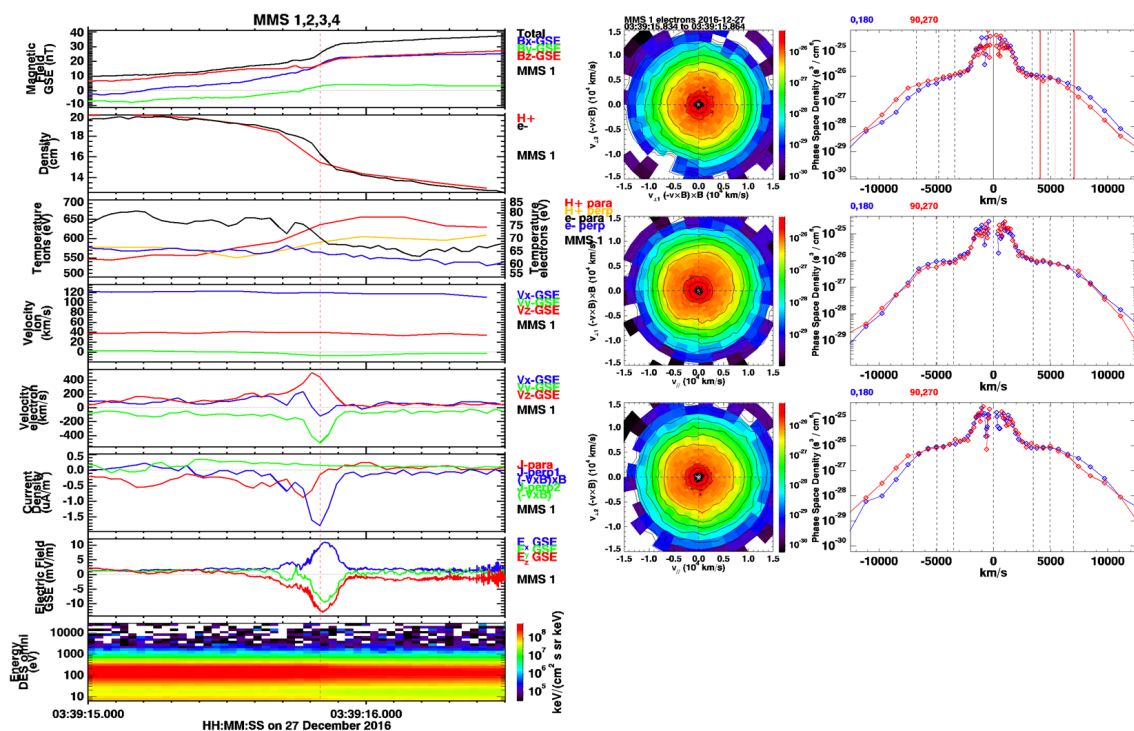
Event #2: Zoom



Event #3: Burst Interval Overview

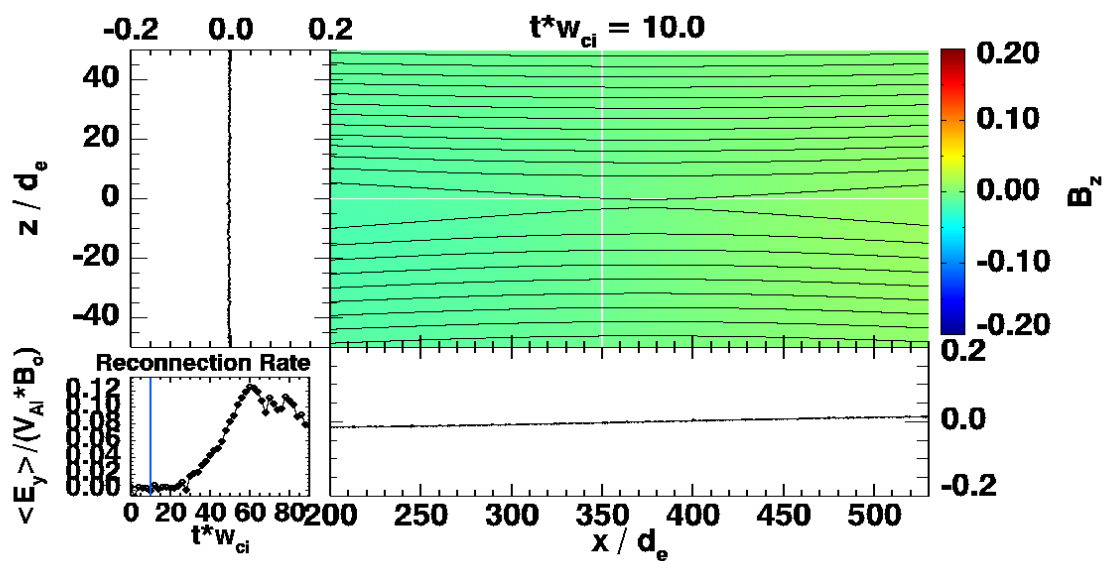


Event #3: Zoom



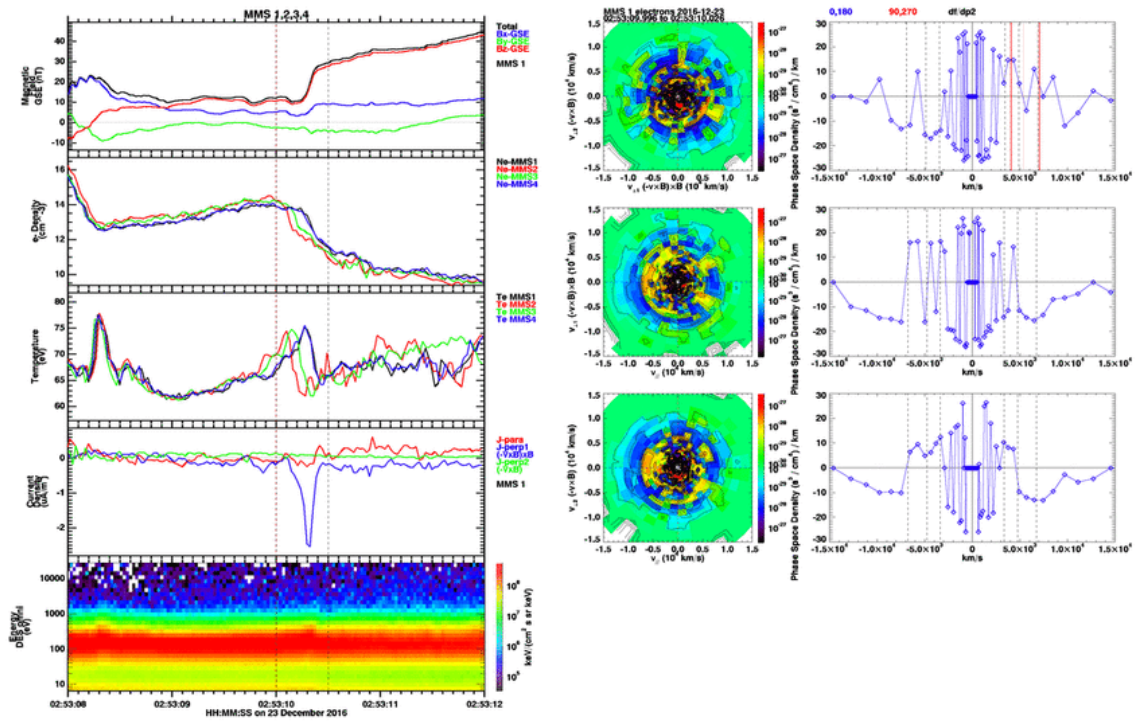
Each thin current sheet is strong ( $J \sim 2 \mu\text{A}/\text{m}^2$ ), is detected within  $\sim 0.5$  seconds, and is embedded within a locally quiet magnetosheath plasma population during MMS's traversal of the magnetopause.

### PIC Simulation Results



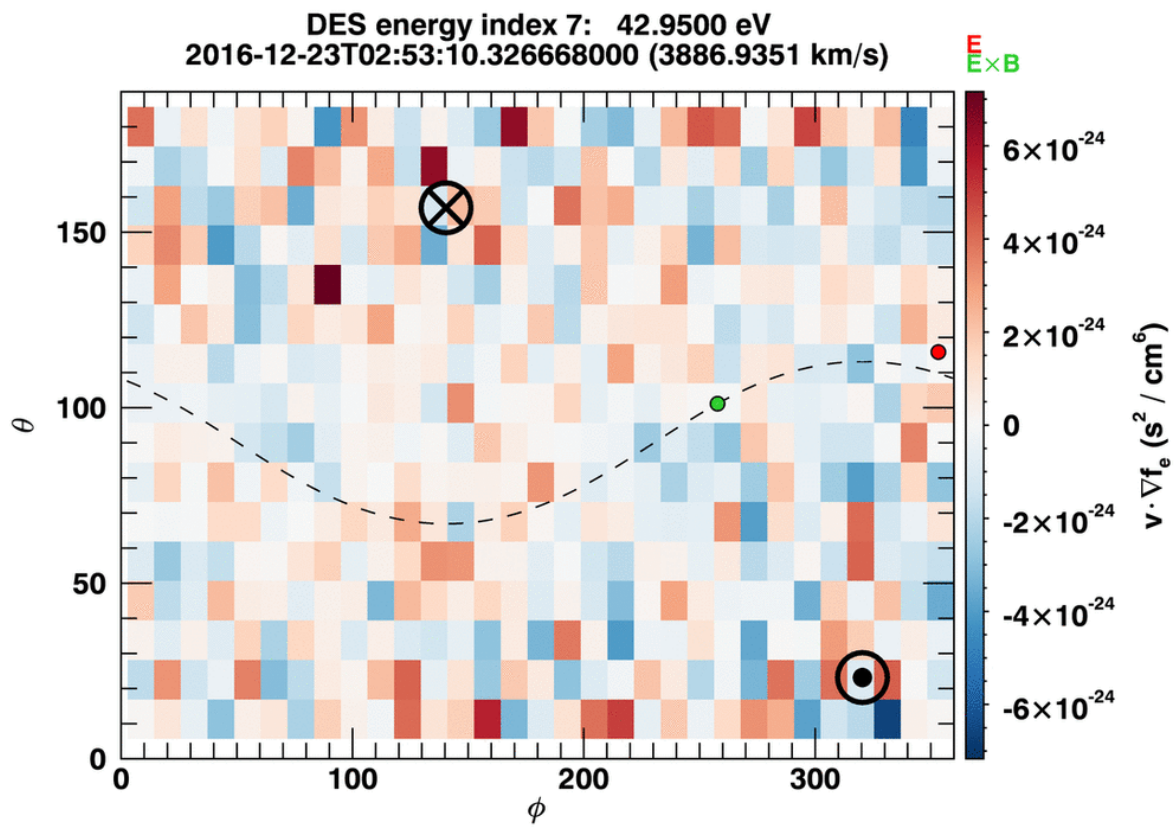
[VIDEO] <https://www.youtube.com/embed/YIibVSDfFmw?feature=oembed&fs=1&modestbranding=1&rel=0&showinfo=0>  
 Electron crescent velocity space structures predicted by particle-in-cell (PIC) simulations of asymmetric magnetic reconnection [Shuster *et al.*, 2017]. For more simulation details, see: Chen *et al.*, 2016.

## VLASOV MEASUREMENTS

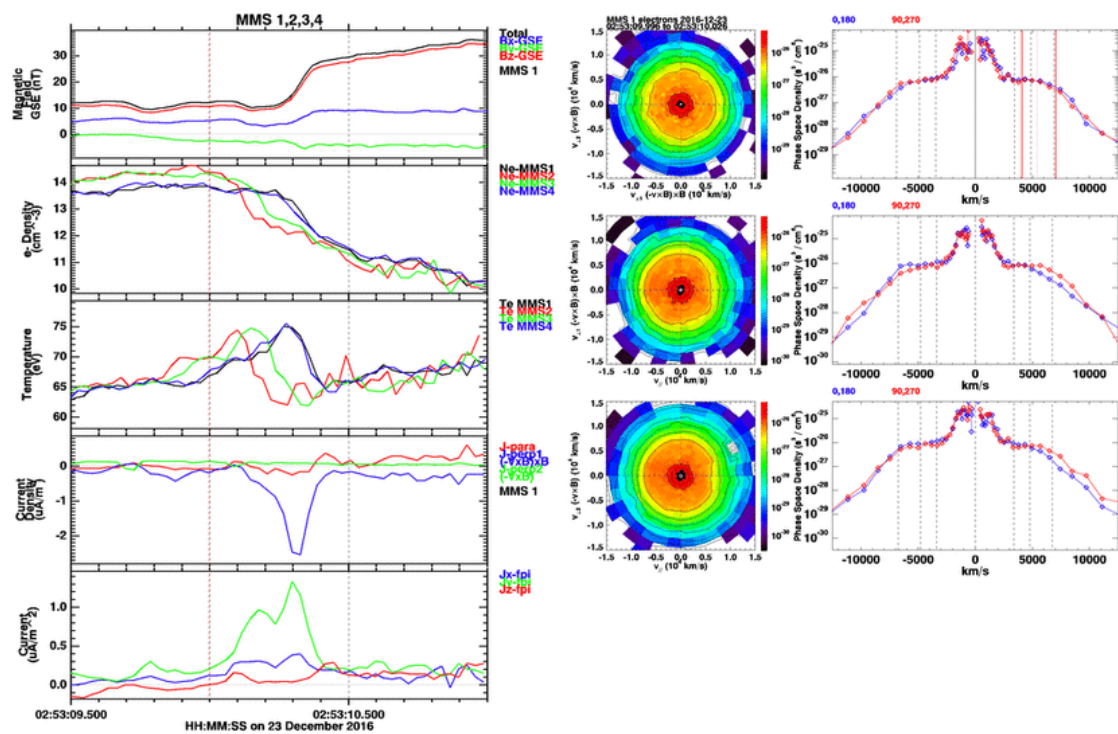


*Vlasov  $\nabla f_{e,12}$  distribution series.*





Energy dependence of  $v \cdot \nabla f_e$



*Electron velocity distribution functions.***Vlasov Measurements**

The animations above show data observed by the four MMS spacecraft on 12/23/2016 (Event #2). The first animation shows data from a sequence of times during a half-second interval for the new quantity  $\nabla f_e$ , the gradient of the electron distribution computed from all four spacecraft (see Methodology). The gradient is projected along the  $\perp_2$  direction, which roughly corresponds to the direction of the density gradient,  $\nabla n$ .

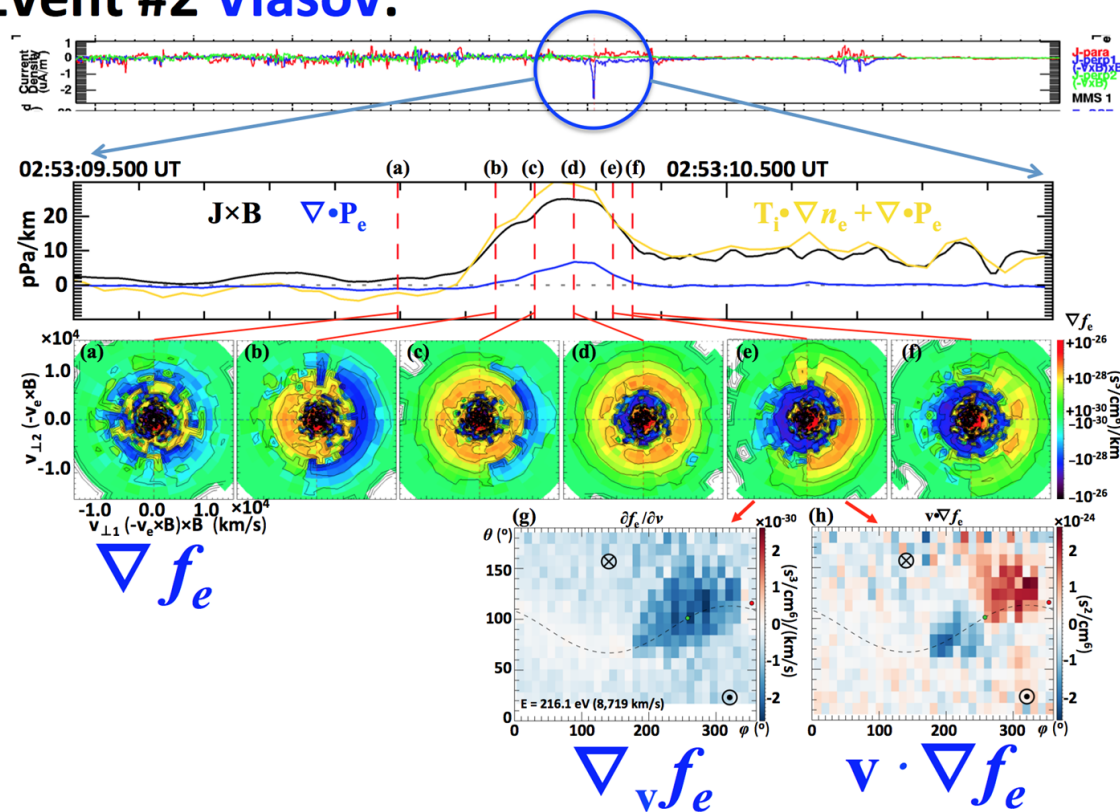
The second animation is of the quantity  $\mathbf{v} \cdot \nabla f_e$  at the time of the crescent distribution, showing the energy dependence of  $\nabla f_e$  structures.

Lastly, the third animation shows a series of electron velocity distribution functions from MMS 1 corresponding to the same time interval of Vlasov distributions shown in the first animation.



## CONCLUSIONS

## Event #2 Vlasov:

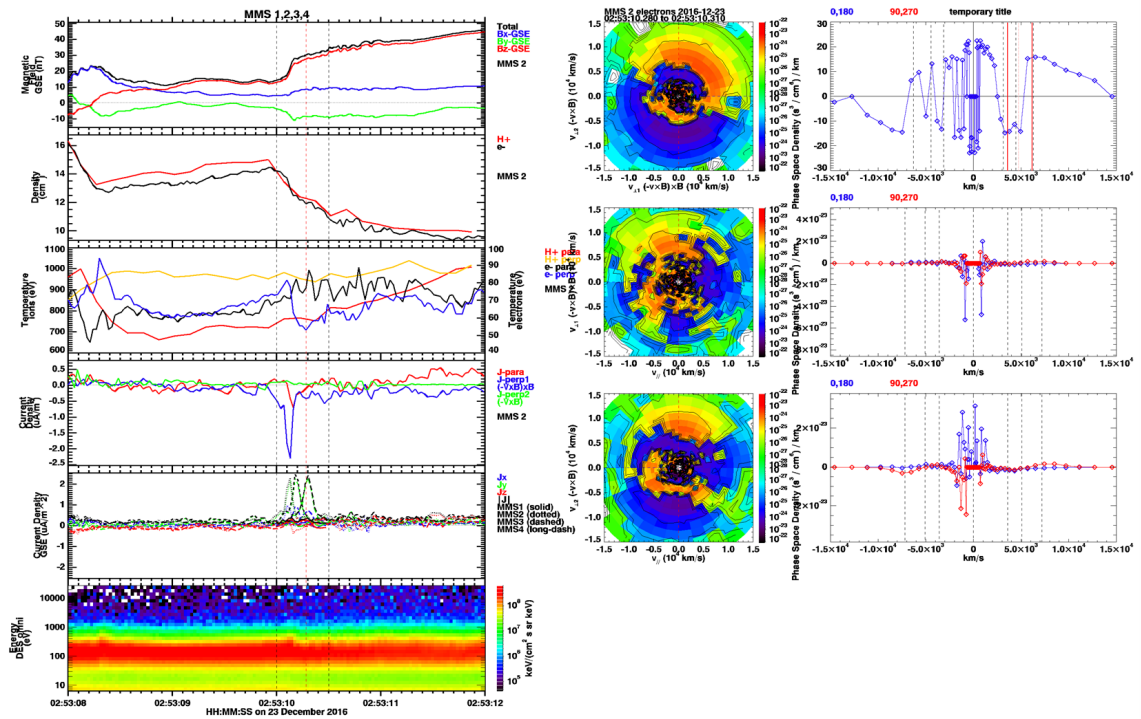


\* First measurements of Vlasov's equation from space enabled by MMS.

\* Evolution of crescent-type structures characteristic of energy conversion within thin current sheets.

\* Bipolar  $\mathbf{v} \cdot \nabla f_e$  signatures associated with the electron-crescent energies.

## FUTURE WORK



*Velocity-space representation of  $\mathbf{v} \cdot \nabla f$ .*

...

- \* Effective visualization techniques for additional  $\nabla f$  terms.
- \* Compare relative contributions of the spatial gradient,  $\nabla f$ , vs. the velocity-space gradient,  $\nabla_v f$ .
- \* Error analysis of phase space density gradients.
- \* Explore Vlasov's equation for ions,  $\nabla_v f_i$ .
- \* Benchmark Vlasov signatures in ambient (quiet) regions vs. active (e.g. EDR) regions.
- \*  $df/dt$  considerations.

## DISCLOSURES

This research was supported in part by NASA grants to the Fast Plasma Investigation, FIELDS team, and the Theory and Modeling Program of the Magnetospheric Multiscale (MMS) mission.

## AUTHOR INFORMATION

### Authors:

Jason R. Shuster<sup>1</sup> (jason.r.shuster@nasa.gov)

Daniel J. Gershman<sup>2</sup>

John Dorelli<sup>2</sup>

Shan Wang<sup>1</sup>

Naoki Bessho<sup>1</sup>

Li-Jen Chen<sup>2</sup>

Daniel Da Silva<sup>3</sup>

Barbara L. Giles<sup>2</sup>

William R. Paterson<sup>2</sup>

...

### Affiliations:

<sup>1</sup>University of Maryland College Park (UMD), College Park, Maryland

<sup>2</sup>NASA Goddard Space Flight Center (GSFC), Greenbelt, Maryland

<sup>3</sup>Trident Vantage Systems, Greenbelt, Maryland

## ABSTRACT

The unprecedented spatiotemporal resolution of the sixty-four dual electron and ion spectrometers comprising the Fast Plasma Investigation (FPI) onboard the four Magnetospheric Multiscale (MMS) spacecraft enables us to compute terms of the Vlasov equation and thus compare MMS measurements directly to kinetic theory. Here we discuss our techniques for determining spatial and velocity-space gradients of the ion and electron distribution function from the skymaps provided by FPI. We present initial results validating and comparing the contributions from  $\partial f / \partial t$ ,  $\mathbf{v} \cdot \nabla f$ , and  $\mathbf{a} \cdot \nabla f$  for a variety of kinetic plasma contexts including both reconnection and non-reconnection events, such as electron diffusion regions (EDRs), magnetic holes, and thin electron-scale current sheets. The ability to resolve gradients of the distribution function motivates comparison of MMS observations to predictions from gyro-kinetic theory and particle-in-cell (PIC) simulations as an approach for determining which physical mechanism is responsible for generating ion and electron crescent distributions observed in association with EDRs and thin boundary layers.

## REFERENCES

### References:

Chen, L.-J., et al. (2016), Electron energization and structure of the diffusion region during asymmetric reconnection, *Geophys. Res. Lett.*, 43, 2405-2412, doi:10.1002/2016GL068243.

Collinson, G. A., J. Dorelli, L. Avanov, G. Lewis, T. Moore, C. Pollock, D. Kataria, R. Bedington, C. Arridge, D. Chornay, U. Gliese, A. Mariano, A. Barrie, C. Tucker, C. Owen, A. Walsh, M. Shappirio, and M. Adrian (2012), The geometric factor of electrostatic plasma analyzers: A case study from the Fast Plasma Investigation for the Magnetospheric Multiscale mission, *Rev. Sci. Instrum.*, 83, 033303, doi:10.1063/1.3687021.

Gurnett and Bhattacharjee (2005), *Introduction to Plasma Physics with Space and Laboratory Applications*, New York: Cambridge University Press, doi:10.1017/CBO9780511809125.

Pollock, C. J., et al. (2016), Fast plasma investigation for magnetospheric multiscale, *Space Sci. Rev.*, 199, 331-405, doi:10.1007/s11214-016-0245-4.

Shuster, J. R., et al. (2017), Hodographic approach for determining spacecraft trajectories through magnetic reconnection diffusion regions, *Geophys. Res. Lett.*, 44, 1625-1633, doi:10.1002/2017GL072570.